Available online at www.sciencedirect.com
ScienceDirect
European Polymer Journal 42 (2006) 2872–2887
EUROPEAN POLYMER JOURNAL
www.elsevier.com/locate/europolj

Small angle neutron scattering and dynamic mechanical thermal analysis of dimethacrylate/epoxy IPNs

Katherine M. Dean [a,b], Wayne D. Cook [a,*], Min Y. Lin [c]

[a] Department of Materials Engineering, P.O. Box 69M, Monash University, Melbourne, Vic. 3800, Australia
[b] Commonwealth Scientific and Industrial Research Organization, 37 Graham Road Highett, Vic. 3190, Australia
[c] National Institute of Standards and Technology (NIST), 100 Bureau Drive, Mail Stop 8562, Gaithersburg, MD 20899-8562, United States

Received 26 May 2005; received in revised form 21 April 2006; accepted 23 April 2006
Available online 14 August 2006

Abstract

Dynamic mechanical thermal analysis (DMTA) and small angle neutron scattering (SANS) have been performed on a number of dimethacrylate (or mono-methacrylate)/diepoxy (or mono-epoxy) interpenetrating polymer networks (IPNs) and semi-IPNs to probe their phase structure. The DMTA behaviour ranged from IPNs that produce one $\tan\delta$ peak, indicative of a single-phase system, to systems that are clearly phase separated, showing two $\tan\delta$ peaks. These results were correlated with the SANS data – samples that showed two $\tan\delta$ peaks also showed scattering in the SANS spectrum. Fitting of the scattering data to the Debye–Bueche scattering model for a phase-separated structure gave a scale to this phase separation of about 180Å. DMTA analysis of the rubbery region of the semi-IPNs revealed that they either had a co-continuous morphology or a matrix phase that was crosslinked.

Keywords: SANS; IPN; DMTA; Phase separation; Epoxy; Dimethacrylate

1. Introduction

The blending of two or more thermosetting monomer systems to form an IPN is one way of optimizing the properties of thermosets. In the original definition, IPNs are a combination of two or more polymers in network form, with at least one of the polymers crosslinked in the presence of the other which causes interlocking of the networks [1–3]. During the polymerization of simultaneous IPNs, either component can be the first to gel [4,5] and the IPN may become thermodynamically unstable resulting in precipitation of a phase rich in either component – the morphology and properties of the resulting IPNs are strongly dependent on these events [1–3]. Ideally the polymerization of the individual components and hence interlocking of the two networks within the IPN should prevent phase separation, although it is documented that entropically driven demixing and phase separation often

* Corresponding author. Tel.: +61 3 99054926; fax: +61 3 99054940.
E-mail address: wayne.cook@eng.monash.edu.au (W.D. Cook).

0014-3057/$ - see front matter © 2006 Elsevier Ltd. All rights reserved.
doi:10.1016/j.eurpolymj.2006.04.013

occur [3,6–8,5] and this process may be enhanced in semi-IPNs [3,8] where the absence of an interlocking structure can allow phase separation. However, if sufficient crosslinking of the components in the IPN occurs before diffusion of the components can occur, phase separation may be largely prevented and a high degree of mixing (close to a single phase morphology) should result [5,9].

There are numerous methods for determining if phase separation has occurred in cured-IPNs. DMTA and DSC are common and useful techniques to study the glass transition temperatures and thus phase separation of IPNs [6,10–13], provided that the individual components of the IPN have clearly defined and well separated T_gs. Small angle neutron scattering has also been used to investigate phase separation in IPNs, providing information about heterogeneities down to a few nanometers and giving information about the type of interface being formed between the phase separated regions [2,14]. Unlike X-rays which are scattered by electrons such that the intensity of scattering increases directly with atomic number, neutrons are scattered by the nuclei of atoms and the strength of this scattering is related to the nuclear structure which is dependant on the atomic mass but not the atomic number [14]. As a consequence, the presence of lighter atoms such as hydrogen can greatly affect the neutron scattering behaviour compared with X-ray scattering. Furthermore, the difference in scattering length of hydrogen and deuterium are significantly different that deuterating a particular phase in a multiphase polymer can give excellent phase contrast [14].

When a polymer sample is placed in the path of a neutron beam, the scattering intensity, $I(Q)$, is the coherent elastic scattering measured at the detector and can be defined as the normalized differential scattering cross section ($d\Sigma(Q)/d\Omega$) where $d\Sigma$ (neutrons s^{-1}) is the number of neutrons scattered per second into a small solid angle. The scattering vector Q is described by Eq. (1) in terms of the wavelength (λ) of the neutron beam and the angle of the scattered beam (θ) from the samples [14,15].

$$Q = \frac{4\pi}{\lambda}\sin\left(\frac{\theta}{2}\right) \tag{1}$$

The amount of scattering of a two-phase system is related to the scattering length of each phase (b_i) and in particular, the difference in scattering length density between each phase (the scattering length, b, per unit volume, v) known as the contrast factor, b_v [14]:

$$b_v = \frac{b_1}{v_1} - \frac{b_2}{v_2} \tag{2}$$

The intensity of scattering is proportional to the square of the contrast factor, b_v between components in a particular system as indicated in Eq. (3). The general expression for the absolute scattering intensities $I(Q)$ in terms of a structure factor $S(Q)$ and form (or shape) factor $P(Q)$ for small angle neutron scattering is given by [16]:

$$I(Q) = \frac{d\Sigma(Q)}{d\Omega} = N_s V_s (b_v^2) P(Q) S(Q) \tag{3}$$

Here $P(Q)$ describes how the scattering intensity is modulated by interference effects between neutrons scattered by different parts of the same scattering center while $S(Q)$ describes the interference effects between neutrons scattered by different scattering centres in the sample and is dependent on the local order in the sample and the interaction potential between scattering components. The term N_s is the number of scattering centres per unit volume and V_s is the volume of the sample illuminated by the neutron beam [14,15]. Several authors have used the Debye–Bueche model [17] to analyze scattering behaviour in immiscible polymer blends [18,19] by determining the correlation length and thus giving a scale to the phase separation. The Debye–Bueche model assumes a random distribution of phases (of differing densities) with different sizes and shapes throughout the scattering volume (V_s). For such a system at low Q, the probability that two points separated by a distance r are in the same phase [17,18,20] is given by:

$$\Gamma(r) = \exp\left(\frac{-r}{\xi}\right) \tag{4}$$

where ξ is the correlation length or average density fluctuation length. The Debye–Bueche model for the scattering intensity can be written as [15–18]:

$$I(Q) = A\left(\frac{1}{(1+\xi^2 Q^2)}\right)^2 + B \tag{5}$$

where $A = 8\pi b_v^2 \phi_1 (1-\phi_1)\xi^3$, ϕ_1 is the volume fraction of phase 1 and B is the background.

In this study, we investigated the extent of phase separation in blends of epoxy resins with methacrylate resins and vinyl ester resins by use of DMTA and SANS.

2. Experimental

Bisphenol-A-diglycidyl-dimethacrylate, (bisGMA, supplied by Esschem Co., USA) and its monomeric analogue-phenyl glycidyl ether methacrylate (PGEMA, synthesised as described elsewhere [21]) were used in this study. The concentration of methacrylate groups in bisGMA was determined by the titration of the α,β-unsaturation with morpholine [22] and the molecular weight of bisGMA was found to be 490 g/mol (compared with the theoretical value of 514 g/mol; $n = 1$), assuming a difunctional monomer. A model vinyl ester resin (VER) was prepared from a solution of bisGMA in 30 wt% styrene monomer (supplied by Huntsman Chemical Company Australia Pty Limited, Australia). Azobisisobutyronitrile (AIBN, supplied by Aldrich Chemicals) was used as the initiator at a concentration of 1 wt% of the bisGMA, PGEMA or VER component. The structures of the reagents are shown in Fig. 1.

The epoxy oligomer was diglycidyl ether of bisphenol-A (DGEBA, Araldite GY-9708-1 supplied by Ciba Geigy). The molecular weight of DGEBA was reported by Ciba Geigy as 372 g/mol and this value was used for the calculations of stoichiometry. A monomeric analogue of DGEBA, 1,2 epoxy-3-phenoxy propane (PGE, supplied by Aldrich) was also investigated. Primary amine curing agents, used in stoichiometric amounts (equimolar NH and epoxy groups) for the cure of DGEBA, were butylamine (BA, supplied by Ajax Chemicals), 1,8-diamino-octane (DAO, supplied by Aldrich), aniline (An, supplied by Unilab) and 4,4′-diaminodiphenyl methane (DDM, supplied by Aldrich). Butylamine and aniline are monomeric analogues of the crosslinking DAO and DDM, respectively. An anionic initiator, 1-methyl imidazole (1-MeI, see Fig. 2, supplied by Ciba Geigy) was also used to cure the epoxy systems at a level of 2 or 5 wt% (as specified). *cis*-1,2 Cyclohexanedicarboxylic anhydride (CHDCA, supplied by Aldrich Chemicals) was also used in stoichiometric ratios (1:1 anhydride to epoxy group) for the cure of the epoxy resin. The epoxy/anhydride cure was accelerated with *N*,*N*-dimethylbenzylamine (DMBA, supplied by Aldrich Chemicals), used at a level of 2 wt% of the total anhydride in the system. The structures of the reagents are shown in Fig. 2.

The liquid aliphatic and aromatic amines BA and An were blended with the epoxy resin at room temperature. Since DDM and DAO are crystalline solids, the diamine and DGEBA were heated separately to the melting point of the diamine (ca. 90 °C and 40 °C, respectively) prior to being mixed for 2 min and rapidly cooled to ambient temperature. The crystalline CHDCA anhydride and the DGEBA were also separately heated to the melting point of the anhydride (32 °C) prior to their mixing and then rapid cooling to ambient temperatures, followed by addition of DMBA and mixing.

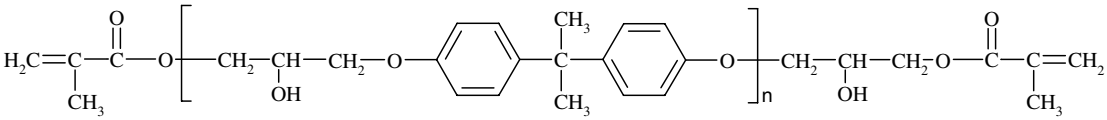

bisGMA

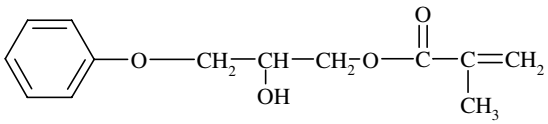

PGEMA

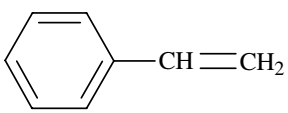

styrene monomer

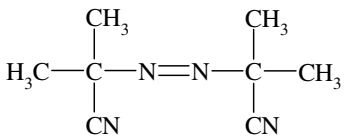

AIBN

Fig. 1. Structures of bisGMA, PGEMA, styrene monomer and AIBN.

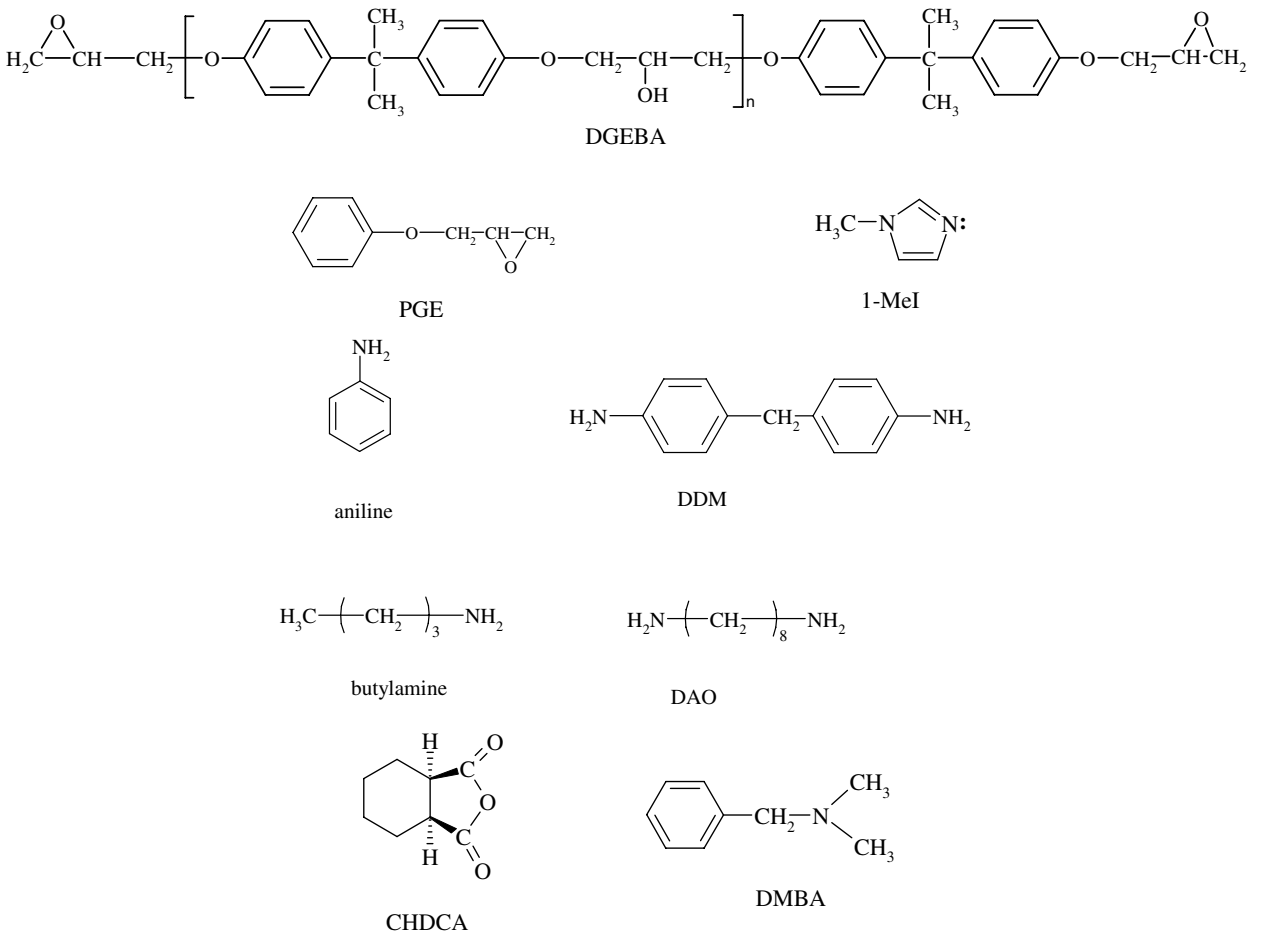

Fig. 2. Structure of DGEBA, PGE, 1-MeI, monofunctional amines and corresponding diamines, CHDCA and DMBA.

The dynamic mechanical behaviour of the fully cured resins and IPNs were measured with a Rheometrics Mark IV DMTA on 1 mm × 6 mm × 20 mm rectangular bars in dual cantilever flexure. The bar samples were cured for 24 h at 70 °C and then post-cured at 180 °C for 2 h (except where otherwise stated). The glass transition temperature was determined by the maximum in $\tan\delta$ at 1 Hz in the dynamic mechanical thermal analysis spectrum. The modulus in the rubbery region was measured at 50 °C above the glass transition temperature of the sample. All DMTA experiments of the fully cured materials were repeated to ensure reproducibility. The error of the modulus was estimated to be ca. ±10–20%.

The densities of the fully cured resin systems were measured using a Micrometrics gas pyncnometer. The pressure used by the fill and purge cycle was 17.5 psi. Approximately 2 g of cured resin (dried at 50 °C under vacuum for 12 h) weighed to an accuracy of ±0.01 mg was sealed in the pressure chamber prior to measurement. An average of 10 measurements of the density were taken of each sample.

SANS experiments were performed at the National Institute of Standards and Technology. The 8 m SANS spectrometer was configured to a sample–detector distance of 3.6 m, off-centre angle of 3.5°, and a central incident neutron wavelength of 12 Å (25% spread). The range of scattering vector (or momentum transfer) probed was $0.006\ \text{Å}^{-1} < Q < 0.09\ \text{Å}^{-1}$. The scattering intensity data was reduced to absolute differential cross section per unit volume (in cm^{-1}) by calibration using a porous silica standard of known differential cross section. The background scattering (without a sample in the beam line), scattering due to stray neutrons and cosmic radiation (beamline blocked with

cadmium-strong neutron absorber) and incoherent scattering (predominantly due to the hydrogen nuclei in the sample) were removed from the scattering data using the IgorPro software package. SANS was performed on plate samples of the resins (thickness of 0.2–0.3 mm). These plates had been machined from 2 mm thick specimens cured for 24 h at 70 °C and then postcured at 170 °C for 2 h (with exception to the VER/AIBN system which was postcured to 150 °C for 2 h).

3. Results and discussion

3.1. DMTA spectra – primary relaxations

Figs. 3–7 show the DMTA spectra and Tables 1 and 2 summarize the results of the DMTA measurements for a range of 50:50 IPNs and their parents based on bisGMA, PGEMA or VER cured with AIBN and of DGEBA or PGE cured with a range of primary amines, imidazoles and anhydride.

DMTA scans of semi- and full-IPNs based on the monomer PGEMA or its crosslinking counterpart bisGMA with the monomer PGE or its crosslinking counterpart DGEBA are shown in Fig. 3. Due to the effect of crosslinks, the T_g of the neat PGEMA/AIBN (45 °C by DSC) rose to 173 °C (by DMTA) for the neat bisGMA/AIBN, while the T_g of the neat PGE/1-MeI (5 °C by DSC) rose to 185 °C (by DMTA) for the neat DGEBA/1-MeI (see Table 1). The corresponding IPNs exhibit a range of dynamical mechanical behaviours. The 50:50 PGEMA/AIBN:DGEBA/1-MeI semi-IPN exhibits a sharp, single transition at 100 °C approximately midway between the T_gs (45 °C and 185 °C) of the parent resins and suggesting a single phase morphology. The 50:50 bisGMA/AIBN:DGEBA/1-MeI IPN also exhibits a single T_g at 177 °C which is midway between the T_gs of the parent resins but in this case the proximity of the parent resin's T_gs is too small to lead to any conclusions about phase separation. In contrast, while the 50:50 bisGMA/AIBN:PGE/1-MeI IPN exhibits a $\tan\delta$ peak at 83 °C which lies between that of PGE/1-MeI (T_g of 5 °C) and the bisGMA/AIBN (T_g of 173 °C) the transition is extremely wide suggesting a wide variation in phase mixing. The difference between the behaviour of the two semi-IPNs is unclear but may be associated with the ability of the linear poly-PGEMA polymer to form hydrogen bonds with the DGEBA/1-MeI network since PGEMA has one hydroxyl group per molecule and the grade of DGEBA used in this study is oligomeric (see Fig. 2) and contains approximately one hydroxy group per 10 molecules. In contrast PGE has no hydroxyl groups to H-bond to the bisGMA network and this may reduce the miscibility of the two.

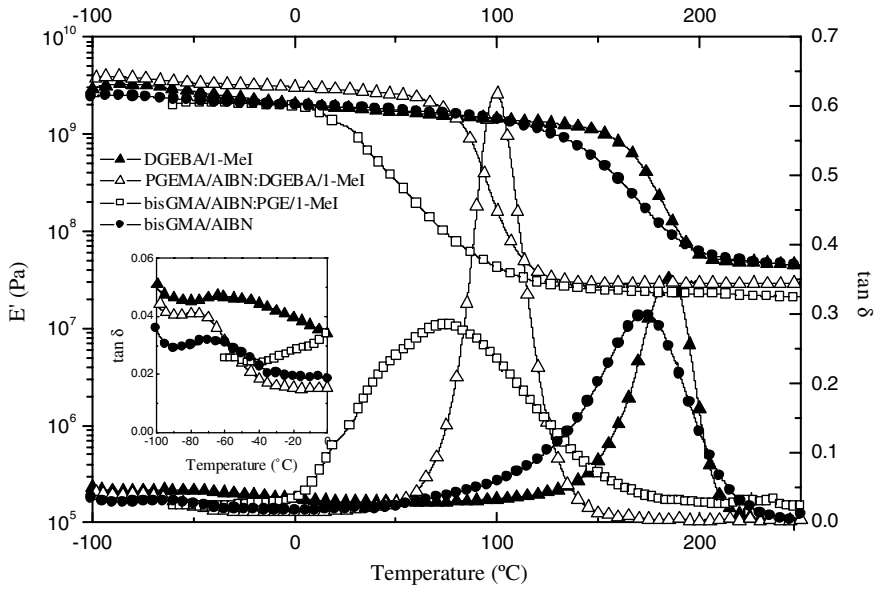

Fig. 3. DMTA scans of DGEBA/1-MeI (2 wt%), bisGMA/AIBN, and the 50:50 semi-IPNs of PGEM/AIBN:DGEBA/1-MeI (5 wt%) semi-IPN and bisGMA/AIBN:PGE/1-MeI (5 wt%).

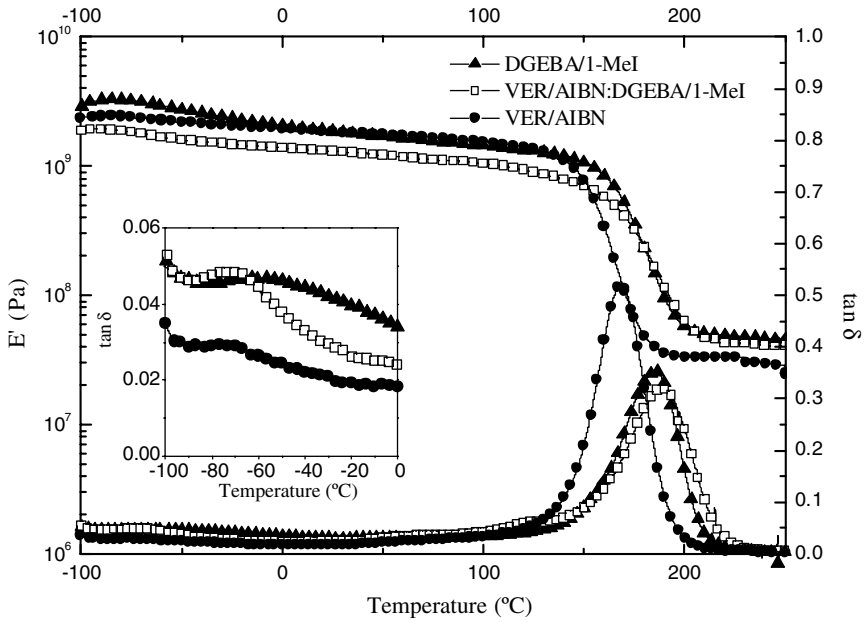

Fig. 4. DMTA scans of DGEBA/2 wt% 1-MeI, VER/AIBN and the corresponding 50:50 IPN.

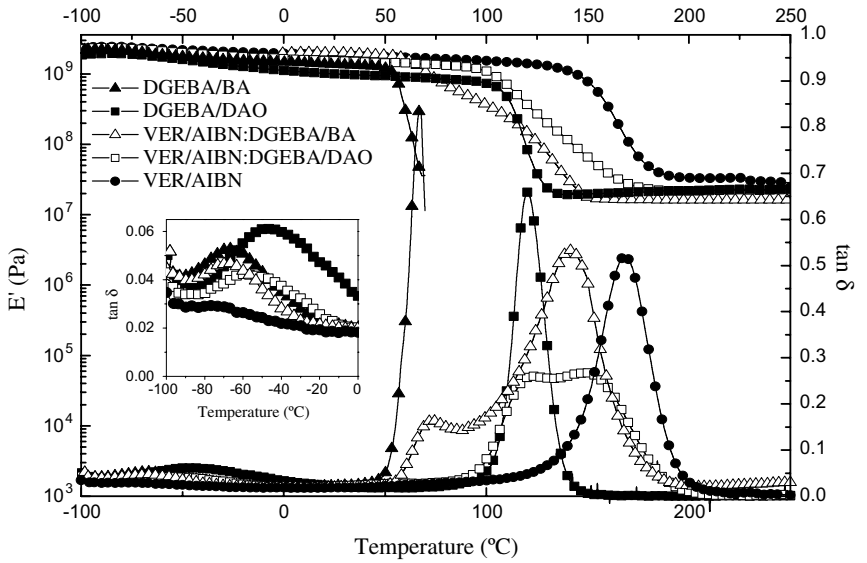

Fig. 5. DMTA scans of DGEBA/BA, DGEBA/DAO, VER/AIBN and corresponding 50:50 IPNs.

The DMTA spectra for VER/AIBN, DGEBA/1-MeI and the resulting IPN are illustrated in Fig. 4. The T_g for the neat VER/AIBN is 169 °C and the T_g for the neat DGEBA/1-MeI is 185 °C. The resulting 50:50 VER/AIBN:DGEBA/1-MeI IPN (see Fig. 4) exhibits a single tan δ peak with a maximum corresponding to a T_g of 189 °C which is close to the T_g of the neat DGEBA/1-MeI, however the close proximities of the T_gs makes discussion of phase separation speculative.

The DMTA spectra for VER/AIBN, DGEBA/BA, DGEBA/DAO and the resulting semi-IPN and full IPN are illustrated in Fig. 5. The neat linear DGEBA/BA shows a single T_g at 67 °C and the neat DGEBA/DAO network shows a single T_g at 119 °C (which is higher than the DGEBA/BA due to the

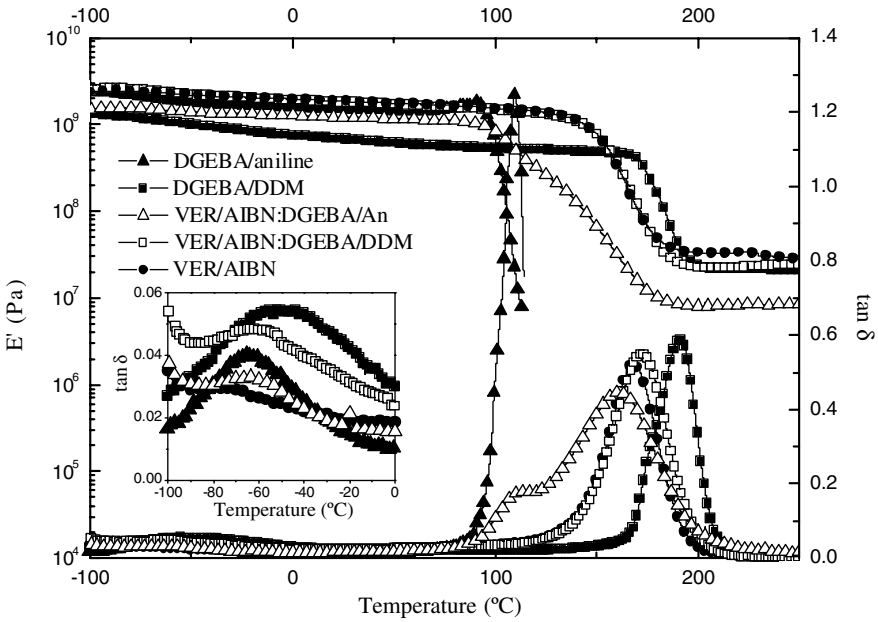

Fig. 6. DMTA scans of DGEBA/An, DGEBA/DDM, VER/AIBN and corresponding 50:50 IPNs.

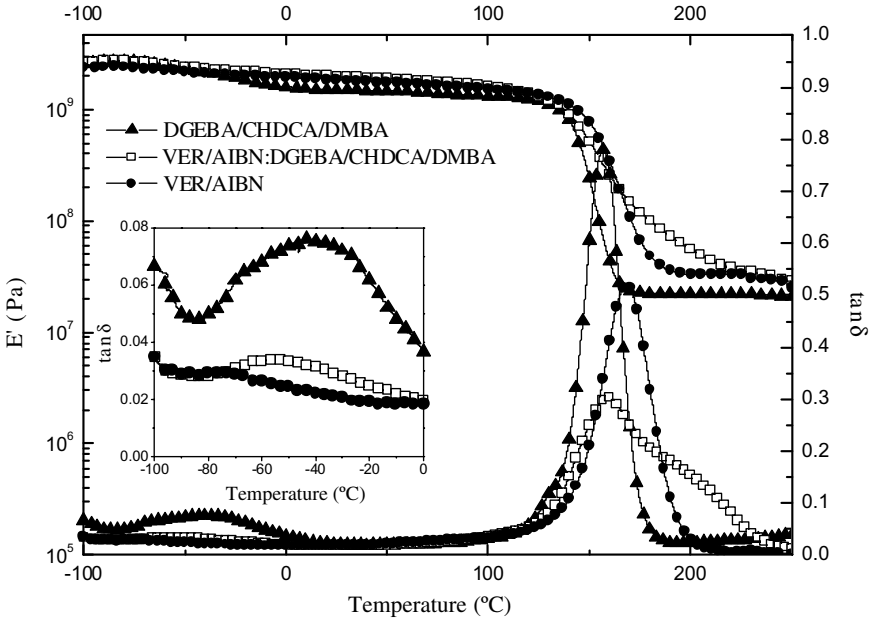

Fig. 7. DMTA scans of DGEBA/CHDCA/DMBA, VER/AIBN and corresponding 50:50 IPN.

presence of crosslinks). The 50:50 VER/AIBN: DGEBA/BA semi-IPN produces two T_gs at 71 °C and 141 °C, the lower T_g due to the epoxy-rich region (neat DGEBA/BA has T_g of 67 °C) and the higher T_g due to the VER-rich region (neat VER/AIBN T_g is 169 °C). There is not much difference in the T_gs of the neat DGEBA/BA and its peak in the IPN which suggests a relatively pure phase. In contrast, the T_g of the VER phase in the IPN is 28 °C lower than in the neat resin. We have previously found [23] that the Michael addition can occur between the methacrylate group and butylamine. However, is appears unlikely that the reduction of the T_gs of the VER component in the VER/

Table 1
DMTA results for parent resins and their IPNs for PGE and PGEM-based systems

System	T_g (°C)	Rubbery modulus (Pa)	β Relaxation (°C)
PGEMA/AIBN	45[a]	Liquid	–
bisGMA/AIBN	173	5×10^7	−70
50:50 PGEMA/AIBN:DGEBA/1-MeI (5 wt%)	100	3×10^7	−75
50:50 bisGMA/AIBN:DGEBA/1-MeI (5 wt%)	177	5×10^7	−60
50:50 bisGMA/AIBN:PGE/1-MeI (5 wt%)	Broad peak at 83 °C with a small shoulder at 18 °C	2×10^7	–
PGE/1-MeI (5 wt%)	5[a]	Liquid	–
DGEBA/1-MeI (2 wt%)	185	5×10^7	−60

[a] T_gs from scanning DSC at 5°/min (DMTA measurements on specimens could not be made readily due to the low T_gs of these materials).

Table 2
DMTA results for parent resins and their IPNs for VER-based systems

System	T_g (°C)	Rubbery modulus (Pa)	β Relaxation (°C)
VER/AIBN	169	3×10^7	−80
VER/AIBN:DGEBA/1-MeI	189	5×10^7	−70
DGEBA/1-MeI	185	5×10^7	−60
VER/AIBN	169	3×10^7	−80
VER/AIBN:DGEBA/BA	Peak 1. 71; Peak 2. 141	2×10^7	−69
VER/AIBN:DGEBA/DAO	Peak 1. 120; Peak 2. 146	2×10^7	−57
DGEBA/BA	67	–	−66
DGEBA/DAO	119	2×10^7	−47
VER/AIBN	169	3×10^7	−80
VER/AIBN:DGEBA/An	Peak 1. 111; Peak 2. 161	1×10^7	−65
VER/AIBN:DGEBA/DDM	171	2×10^7	−63
DGEBA/An	109	–	−64
DGEBA/DDM	189	2×10^7	−50
VER/AIBN	169	3×10^7	−80
VER/AIBN:DGEBA/CHDCA/ DMBA	157 with a large shoulder	2×10^7	−54
DGEBA/CHDCA/ DMBA	159	2×10^7	−41

AIBN:DGEBA/BA semi-IPN is solely caused by the Michael addition because this reaction would cause an epoxy–amine imbalance and also reduce the T_g of the epoxy phase, but this is not observed. The depression in T_g of the VER-rich phase may be also caused by some phase mixing of the low T_g DGEBA/BA with the VER-rich phase. The 50:50 VER/AIBN:DGEBA/DAO full-IPN also exhibits two T_gs of 120 °C and 146 °C, the lower T_g at 120 °C can be assigned to the epoxy (neat DGEBA/DAO has T_g of 119 °C) while the higher T_g is due to the VER-rich phase (neat VER/AIBN T_g is 169 °C). As found for the BA based IPN, there does not appear to be much difference in the T_g of the epoxy whether neat or in the IPN system, however the VER T_g is 23 °C lower in the IPN compared with the neat resin and this may also be due to Michael addition and/or phase mixing in the VER-rich phase, as discussed above.

The DMTA spectra for VER/AIBN, DGEBA/An, DGEBA/DDM and the resulting semi-IPN and full IPN are illustrated in Fig. 6. The neat linear DGEBA/An shows a single T_g at 109 °C and the neat crosslinking DGEBA/DDM shows a single T_g at 189 °C (which is higher than that of DGEBA/An due to the presence of crosslinks). The resulting semi-IPN produces two T_gs at 111 °C and 161 °C, the lower corresponding to the T_g of the DGEBA/An and the higher corresponding to the VER/AIBN. Similar to the aliphatic amine-based IPNs, the T_g of the aromatic amine/epoxy-rich phase in the semi-IPN was similar to that of the neat epoxy, indicating a relatively pure phase. The T_g for the VER phase was 48 °C lower in the 50:50 VER/AIBN:DGEBA/An semi-IPN compared to the neat VER, either due to Michael addition and/or phase mixing as discussed above. The decrease in T_g for the VER component in the

50:50 VER/AIBN:DGEBA/An IPN was significantly larger than that found with the aliphatic amine based IPN. This cannot be due to enhanced Michael addition because the aromatic amine is less reactive with methacrylate than the aliphatic amine [23]. Perhaps this difference results from a greater miscibility of the DGEBA/An with the VER-rich phase due to their similar aromatic structures. The 50:50 VER/AIBN:DGEBA/DDM full-IPN appears to have a single T_g of 171 °C, however, the small difference in T_g of the parent resins in the DDM base IPN (VER/AIBN – 169 °C and DGEBA/DDM – 189 °C) makes it difficult to determine whether a two-phase system existed. Thus, based solely on the DMTA data, the 50:50 VER/AIBN:DGEBA/DDM IPN may have partial phase separation or be completely miscible.

The DMTA spectra for VER/AIBN, DGEBA/CHDCA and the corresponding IPN is shown in Fig. 7. The neat DGEBA/CHDCA shows a single T_g at 157 °C and the neat VER/AIBN has a T_g of 169 °C. The resulting 50:50 VER/AIBN:DGEBA/CHDCA IPN produces a single T_g at 159 °C with a shoulder on the higher temperature side of the peak. It is not clear why this shoulder is at a higher temperature than the parent resins – perhaps the CHDCA anhydride reacts with the hydroxy groups of the bisGMA component of the VER and raises the crosslink density and T_g. However, the broad transition region of this IPN suggests some degree of phase separation.

3.2. Rubbery modulus

It is well documented that the modulus in the rubbery region is related to the crosslink density; however for materials with a high crosslink density, deviations from a linear relationship have been observed [24]. Given that the DMTA technique does not usually give precise modulus results (due to specimen clamping effects), the rubbery moduli values reported here see Table 2) give only a qualitative indication of the crosslink density. The rubbery modulus of the 50:50 bisGMA/AIBN:DGEBA/1-MeI IPN is 5×10^7 Pa which is the same (within experimental error) as that for DGEBA/1-MeI (5×10^7 Pa) and bisGMA/AIBN (5×10^7 Pa). The values of rubbery modulus for the 50:50 PGEMA/AIBN:DGEBA/1-MeI (3×10^7 Pa) and 50:50 bisGMA/AIBN:PGE/1-MeI (2×10^7 Pa) are low (as expected) due to the uncrosslinked PGEMA/AIBN and PGE/1-MeI components.

The rubbery modulus of the 50:50 VER/AIBN:DGEBA/1-MeI IPN is 5×10^7 Pa which is within experimental error of that for DGEBA/1-MeI (5×10^7 Pa) and VER/AIBN (3×10^7 Pa). The VER/AIBN:DGEBA/DAO (2×10^7 Pa), VER/AIBN:DGEBA/DDM (2×10^7 Pa) and VER/AIBN:DGEBA/CHDCA (2×10^7 Pa) IPNs also all exhibited rubbery modulus values between those recorded for the parent resins. The values of rubbery modulus for the 50:50 VER/AIBN:DGEBA/BA (2×10^7 Pa) and VER/AIBN:DGEBA/An (1×10^7 Pa) IPNs are low (as expected) due to the uncrosslinked DGEBA/BA and DGEBA/An components.

The presence of a rubbery plateau for the PGEMA/AIBN:DGEBA/1-MeI IPN is not surprising because it is a single phase system and the epoxy component is crosslinked. However, for the two-phase BA, An, and PGE-based IPNs, the presence of a rubbery plateau shows that the structure either consists of a co-continuous morphology with the two phases interpenetrating with one another or of uncrosslinked epoxy domains dispersed in a continuous crosslinked VER-rich phase.

3.3. Secondary DMTA spectra relaxations

The secondary (or β) relaxation in the neat bisGMA (−70 °C) has been assigned to localized molecular motion of the methacrylate group [25], however it may also be due to the glyceryl segment (–CH_2–CH(OH)–CH_2–O– as shown in Fig. 1) which also exists in diamine-cured DGEBA [26,27]. The β relaxation in the neat DGEBA/1-MeI (−60 °C, see Table 2) is not likely to be due to the glyceryl segments because the anionic polymerization does not generate glyceryl units and only a small fraction exist in the DGEBA/1-MeI network due to the oligomeric impurities in DGEBA (see Fig. 2). Therefore, this relaxation may be caused by the localized motion of the bisphenol-A group [26,27]. The broad β relaxations of the 50:50 bisGMA/AIBN:DGEBA/1-MeI (−60 °C) is close to the average of its parent resins and the 50:50 PGEMA/AIBN:DGEBA/1-MeI IPN also exhibited a broad β relaxation in this region. The neat VER exhibits a small β relaxation (at −80 °C) which, by analogy to the β relaxation in the neat bisGMA, may be associated with localized molecular motion of the methacrylate group [25] or the glyceryl segment which also exists in diamine-cured DGEBA [26,27]. It is unlikely to be the low temperature

relaxation of polystyrene because this occurs between −100 °C and −140 °C [25]. The β relaxation of the 50:50 VER/AIBN:DGEBA/1-MeI IPN (at −70 °C) appears to be a combination of the β relaxations for the two parent resins.

The β relaxation for the DGEBA/BA (at −66 °C), DGEBA/DAO (at −47 °C), DGEBA/An (at −64 °C) and DGEBA/DDM (at −50 °C) may be partly due to the motion of the glyceryl (–CH_2–CH(OH)–CH_2–O) segment in the reacted DGEBA unit or could be caused by motion of the bisphenol-A group [26,27]. The aromatic and aliphatic-amine based IPNs exhibit β relaxations close to an average of the two parent resins.

The β relaxation for the DGEBA/CHDCA (at −41 °C) may be due to a combination of the motions of the bisphenol-A group [27] and the diester segment from the anhydride [28]. The 50:50 VER/AIBN:DGEBA/CHDCA IPN exhibited a β relaxation (−54 °C) which occurs between the values measured for the parent resins.

4. Small angle neutron scattering (SANS)

A summation of the scattering due to each atom [14] within each component of the IPN was calculated and the scattering length per repeat unit for each component sub-unit is listed in Table 3. The scattering length (b_i) for each component and density of the neat resin (see Table 3) were used to calculate the scattering length density for the neat resins:

$$\text{scattering length density} = \left(\frac{\rho \times \text{Avogadro's number}}{\text{MW of repeat unit}}\right) \times (\Sigma b_i)_{\text{component}} \quad (6)$$

In some cases the difference in scattering length density of the components of an IPN is close to the threshold of observable scattering; for example the scattering length density for the VER/AIBN is $148 \times 10^8\ \text{cm}^{-2}$ which is very close to DGEBA/CHDCA/DMBA ($155 \times 10^8\ \text{cm}^{-2}$), hence even if the system was phase separated, the difference in scattering length density ($b_v = 14 \times 10^8\ \text{cm}^{-2}$) may be too small for scattering to be observed.

The spectra of the scattering intensity $I(Q)$ versus the scattering vector Q, for a series of IPNs and their parent resins are shown in Figs. 8–13. As expected, the scattering from the neat resins is very small which is consistent with a homogeneous structure. The 50:50 VER/AIBN:DGEBA/CHDCA/DMBA IPN (Fig. 11) also exhibits minimal scattering. As shown previously, the DMTA traces of VER/AIBN:DGEBA/CHDCA/DMBA indicated a two-phase structure. Thus, it appears that either a value for b_v of less than $14 \times 10^8\ \text{cm}^{-2}$ is too small to detect a two-phase structure by SANS, or that styrene (which has a lower value for b_v than bisGMA) has diffused into the epoxy-rich phase, thus reducing the difference in scattering length density. The scattering shown in Fig. 13 for the VER/AIBN:DGEBA/An semi-IPN suggests that it is phase-separated, which is consistent with its DMTA spectra (Fig. 6). Therefore, for the VER/AIBN:DGEBA/An semi-IPN, the theoretical value of $20 \times 10^8\ \text{cm}^{-2}$ for the difference in scattering length density is sufficient to produce observable scattering. Similarly, the VER/AIBN:DGEBA/DDM IPN shows strong scattering in the SANS plot (Figs. 10 and 13), because it is a phase-separated IPN with a sufficiently large value of b_v ($28 \times 10^8\ \text{cm}^{-2}$) – the inability to detect two T_gs in this system (Fig. 6) is due to the close proximity of the parent resins T_gs. The failure to observe significant scattering in the VER/AIBN:DGEBA/1-MeI IPN (Fig. 8), despite the large value of b_v ($38 \times 10^8\ \text{cm}^{-2}$) suggests that this system is not phase separated or that styrene has diffused into the epoxy-rich phase and thus reduced the difference in scattering length density, however the latter hypothesis is not consistent with the behaviour of VER/AIBN:DGEBA/An and VER/AIBN:DGEBA/DDM. The 50:50 VER/

Table 3
Summary of density and scattering length density for all the neat resins

Component	Density (g/cm^3)	Scattering length density per repeat unit (cm^{-2})	Difference in scattering length density between the component and VER/AIBN (cm^{-2})
DGEBA/1MeI	1[a]	129×10^8	38×10^8
DGEBA/DAO	1.20	126×10^8	44×10^8
DGEBA/BA	1.18	117×10^8	62×10^8
DGEBA/DDM	1.19	162×10^8	28×10^8
DGEBA/An	1.18	158×10^8	20×10^8
DGEBA/CHDCA/DMBA	1.20	155×10^8	14×10^8
VER/AIBN	1.17	148×10^8	0
Styrene	1[a]	135×10^8	–
bisGMA	1[a]	123×10^8	–

[a] Estimated.

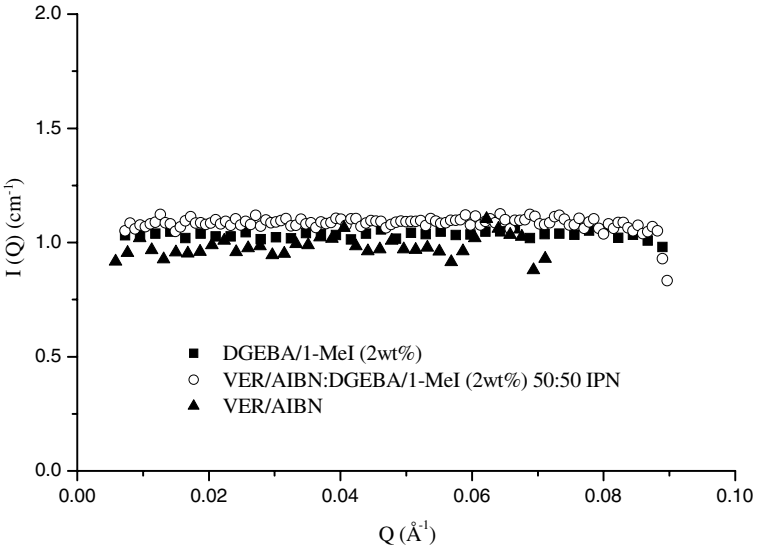

Fig. 8. Scattering intensity $I(Q)$ versus scattering vector Q for DGEBA/1-MeI (2 wt%), VER/AIBN and the 50:50 IPN.

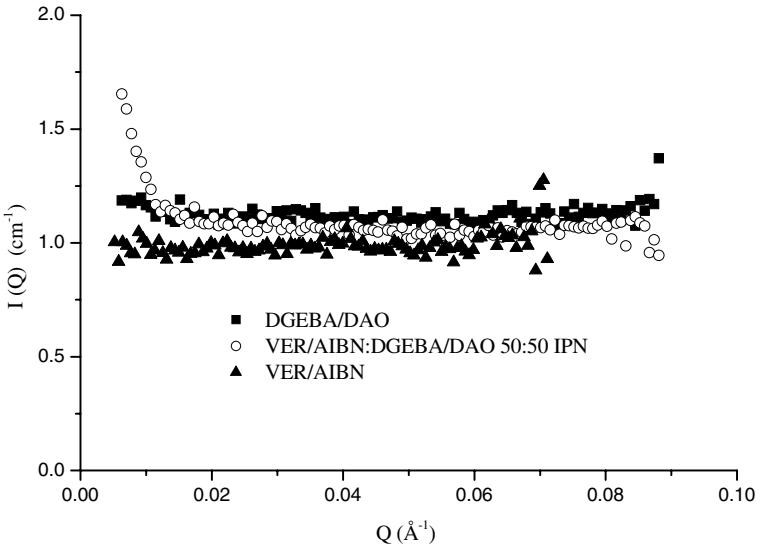

Fig. 9. Scattering intensity $I(Q)$ versus scattering vector Q for DGEBA/DAO, VER/AIBN and the 50:50 IPN.

AIBN:DGEBA/DAO IPN (Figs. 9 and 12) and to a greater extent the 50:50 VER/AIBN:DGEBA/BA semi-IPN (Fig. 12) produced scattering indicative of a two phase system due to the large difference in scattering length density from the VER/AIBN resin ($b_v = 44 \times 10^8$ cm^{-2} and 62×10^8 cm^{-2}, respectively) and this phase separation is confirmed by the DMTA data (see Fig. 5).

The scattering behaviour of the VER/AIBN:DGEBA:BA, VER/AIBN:DGEBA:DAO VER/AIBN:DGEBA:An and VER/AIBN:DGEBA:DDM IPNs was fitted to the Deybe–Bueche model [17,15,20] (see Eq. (5)) by minimization of the variant over the Q range from 0.006 to 0.03 Å^{-1}, as shown in Figs. 12 and 13 and values of the correlation length in each IPN are listed in Table 3. The scattering data from the 50:50 IPNs of VER/AIBN:DGEBA/BA IPN and VER/AIBN:DGEBA/DAO IPN fits the Deybe–Bueche reasonably well giving values for ξ of 181 ± 4Å and 151 ± 12Å, respectively. Similarly, the scattering data from the 50:50 VER/AIBN:DGEBA/An IPN

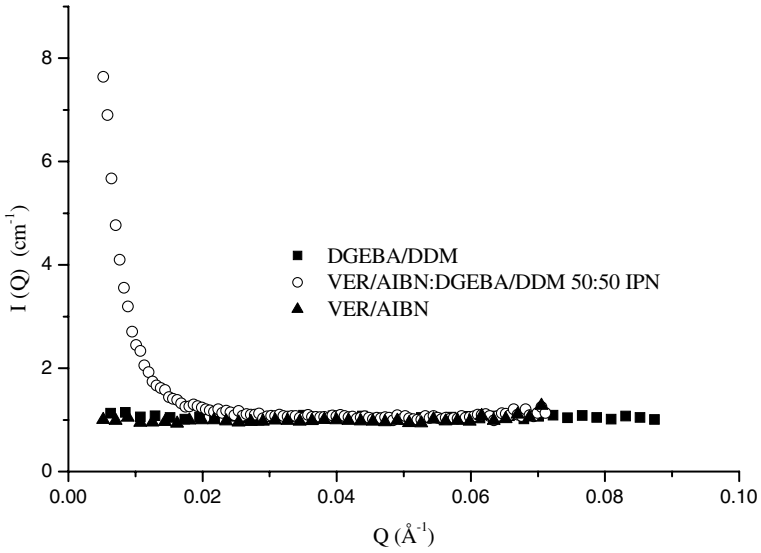

Fig. 10. Scattering intensity $I(Q)$ versus scattering vector Q for DGEBA/DDM, VER/AIBN and the 50:50 IPN.

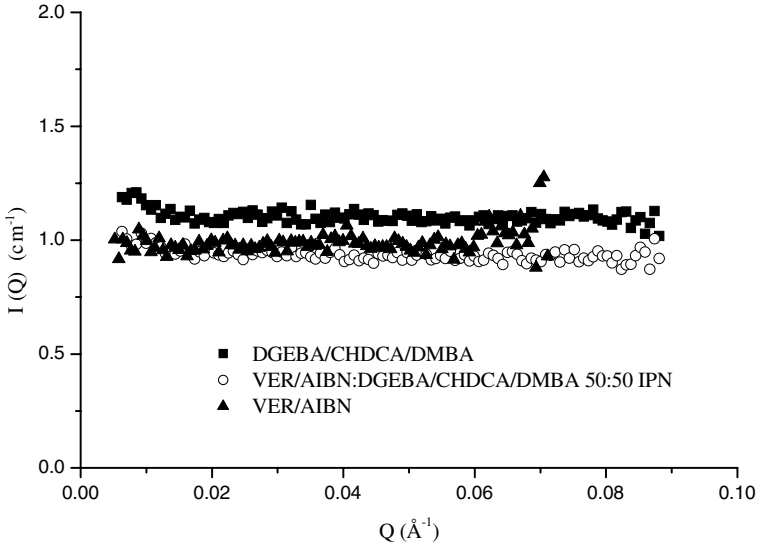

Fig. 11. Scattering intensity $I(Q)$ versus scattering vector Q for DGEBA/CHDCA/DMBA, VER/AIBN and the 50:50 IPN.

and 50:50 VER/AIBN:DGEBA/DDM IPN produced good fits to the Deybe–Bueche equation with correlation lengths of 186 ± 8Å and 184 ± 6Å, respectively. The sizes of these domains are very small (smaller than the wavelength of light) and so the samples are not visually opaque.

According to the Debye–Bueche model (Eq. (5)), the parameter A in Table 4 is equal to $8\pi b_v^2 \phi_1(1-\phi_1)\xi^3$, so that $A/(b_v^2\xi^3)$ should be proportional to $\phi_1(1-\phi_1)$ and give a measure of the extent of phase separation. If phase mixing does not occur, the theoretical values of b_v listed in Table 3 can be used. On this basis, the quantity $A/(b_v^2\xi^3)$ is listed in Table 4. For the VER/AIBN:DGEBA:DAO IPN, the epoxy and dimethacrylate networks form in a similar time period so it is likely that the network interlocking will reduce the extent of phase separation [29]. If this occurs then it is not surprising that the measured domain size (ξ) is smaller than for the other systems. Additionally, the interlocking of the VER/AIBN and DGEBA:DAO networks would reduce the purity of the phases so that the

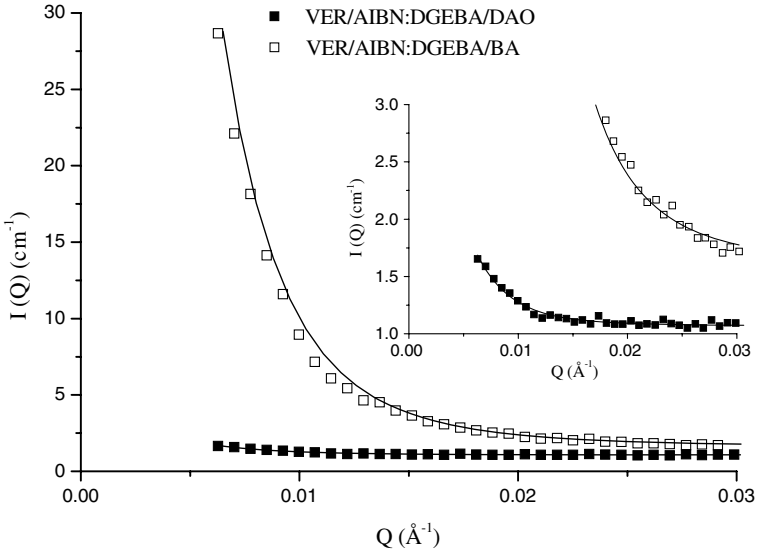

Fig. 12. Deybe–Bueche fitting of 50:50 VER/AIBN:DGEBA:BA and 50:50 VER/AIBN:DGEBA:DAO scattering data.

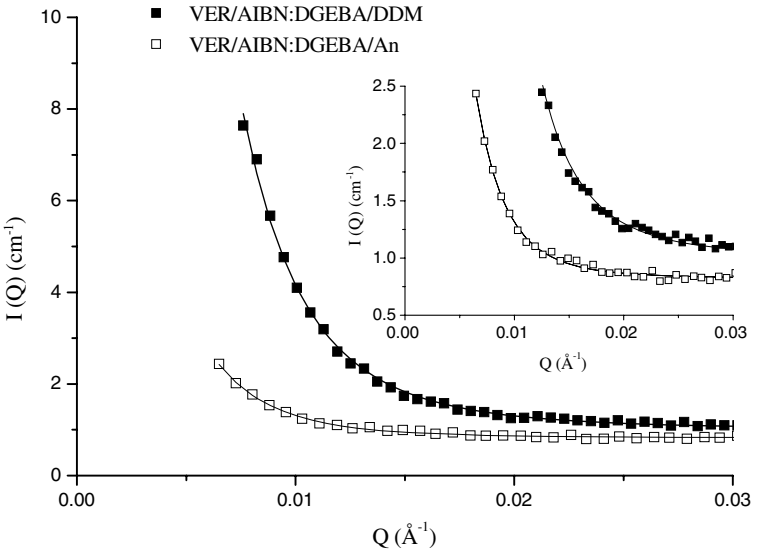

Fig. 13. Deybe–Bueche fitting of 50:50 VER/AIBN:DGEBA:An and 50:50 VER/AIBN:DGEBA:DDM scattering data.

Table 4
Deybe–Bueche parameters for 50:50 VER/AIBN:DGEBA:BA, 50:50 VER/AIBN:DGEBA:DAO, 50:50 VER/AIBN:DGEBA:An and 50:50 VER/AIBN:DGEBA:DDM

System	ξ (Å) Fitted values	A (cm^{-1}) Fitted values	$A/(b_v^2\xi^3)$ (cm^3 Å^3)
VER/AIBN:DGEBA:BA	181 ± 4	155 ± 8	0.68×10^{-24}
VER/AIBN:DGEBA:DAO	151 ± 12	2.2 ± 0.4	0.033×10^{-24}
VER/AIBN:DGEBA:An	186 ± 8	10 ± 1	0.39×10^{-24}
VER/AIBN:DGEBA:DDM	184 ± 6	61 ± 6	1.24×10^{-24}

value of b_v used to calculate the quantity $A/(b_v^2\xi^3)$ would be an overestimate (since it assumes complete phase separation) and the quantity $A/(b_v^2\xi^3)$ would be underestimated, thus explaining why it is so

much smaller than for the VER/AIBN:DGEBA:BA semi-IPN. In contrast, the VER/AIBN:DGEBA:BA blend is a semi-IPN and so provided the DGEBA/BA chains can diffuse readily, larger domains with a greater level of phase separation should occur, as indicated by the ξ and $A/(b_v^2\xi^3)$ data in Table 4. The value of $A/(b_v^2\xi^3)$ for the VER/AIBN:DGEBA:An and VER/AIBN:DGEBA:DDM IPNs are similar to that for the VER/AIBN:DGEBA:BA semi-IPN indicating extensive phase separation. The epoxy component in the VER/AIBN:DGEBA:An and VER/AIBN:DGEBA:DDM IPNs polymerize after the formation of the VER/AIBN network and this should favour phase separation [29]. Like the VER/AIBN:DGEBA:BA blend, the VER/AIBN:DGEBA:An blend is a semi-IPN and so phase separation would be expected to be more complete. However, this hypothesis is not in agreement with the values of $A/(b_v^2\xi^3)$ in Table 4 – the value of $A/(b_v^2\xi^3)$ is greater for VER/AIBN:DGEBA:DDM but the assumed value for b_v would be an underestimated if phase-mixing was significant as it should be for a full-IPN.

5. Conclusions

A range of 50:50 IPNs with differing morphologies have been produced. The phase structure, as observed by SANS and/or DMTA, is summarized in Table 5. The blends comprise the clearly phase separated IPNs which showed two T_gs by DMTA (bisGMA/AIBN:PGE/1-MeI) and excess small angle neutron scattering (50:50 VER/AIBN:DGEBA/An, 50:50 VER/AIBN:DGEBA/BA and the 50:50 VER/AIBN:DGEBA/DAO). A second group is the 50:50 VER/AIBN:DGEBA/DDM IPN whose phase structure cannot be determined by DMTA analysis (a single, possibly overlapped T_g is observed) but which show obvious small angle neutron scattering; or the 50:50 VER/AIBN:DGEBA/CHDCA/DMBA IPN which only shows a small level of neutron scattering but which exhibits a peak with a shoulder in the DMTA spectrum. A third group of IPNs are those that appear to be single phase materials, showing a single T_g by DMTA (PGEMA/1-MeI:DGEBA/1-MeI) and no small angle neutron scattering (VER/AIBN:DGEBA/1-MeI). The ability to detect phase separation by the DMTA and SANS techniques depends to a certain extent on how different the parent polymers are from one another – in particular this applies to the bisGMA/AIBN:DGEBA/1-MeI IPN because the difference in the Ts of the components is too small to determine phase separation and the predicted scattering density difference (calculable for the data in Table 3 is too small to be detectable).

These results indicate that the phase structure of IPNs is strongly dependent on the miscibility of the components constituting the IPN and also the polymerization kinetics of those components. The backbone monomers chosen in this work (bisGMA and DGEBA) were chosen to be similar in structure to reduce the thermodynamic binary interaction parameter and thus increase the miscibility of the polymers, however it may be noted that small changes in structure can have a significant effect on the resulting IPN morphology. For example, the bisGMA/AIBN:DGEBA/1-MeI semi-IPN is miscible but the bisGMA/AIBN:PGE/1-MeI semi-IPN is not. In addition, IPNs containing BA, DAO, An and DDM as curing agents for DGEBA epoxy appear to cause a two-phase morphology in contrast to the single phase structure of VER/AIBN:DGEBA/1-MeI.

Table 5
Summary of evidence for phase separation in the IPNs

System	ΔT_g (parent resins) (°C)	Two T_gs by DMTA	Scattering density difference (cm^{-2})	Observed SANS	Phase separation
bisGMA/AIBN:DGEBA/1-MeI	12	No	–	–	Indeterminate
bisGMA/AIBN:PGE/1-MeI	168	Yes	–	–	Yes
PGEMA/1-MeI:DGEBA/1-MeI	140	No	–	–	No
VER/AIBN:DGEBA/1-MeI	16	No	38×10^8	No	No
VER/AIBN:DGEBA/BA	102	Yes	62×10^8	Yes	Yes
VER/AIBN:DGEBA/DAO	40	Yes	44×10^8	Yes	Yes
VER/AIBN:DGEBA/An	50	Yes	20×10^8	Yes	Yes
VER/AIBN:DGEBA/DDM	20	No	28×10^8	Yes	Yes
VER/AIBN:DGEBA/CHDCA/DMBA	10	Yes (a peak with a shoulder)	14×10^8	Yes (borderline)	Yes

Four systems which showed significant small angle neutron scattering were analysed with the Deybe–Bueche model. The correlation calculated length (ξ) was 181 ± 4Å, 151 ± 12Å, 186 ± 8Å and 184 ± 6Å for the 50:50 VER/AIBN:DGEBA/BA IPN, 50:50 VER/AIBN:DGEBA/DAO IPN, 50:50 VER/AIBN:DGEBA/An IPN and 50:50 VER/AIBN:DGEBA/DDM IPN, respectively. The lower correlation length for the VER/AIBN:DGEBA/DAO IPN may be due to a reduction in phase separation due to the near simultaneous interlocking of the two networks during cure. This is not observed for the VER/AIBN:DGEBA/DDM IPN in which the correlation length is similar to that of the VER/AIBN:DGEBA/An semi-IPN perhaps because the slower cure of the epoxy component and the reduction in entropy during the cure of the DGEBA/DDM component causes phase separation before the interlocking of the two networks can occur.

Acknowledgements

The authors would like to thank Robert Knott, Howard Hanley (ANSTO) and David Sutton (CRC for Polymers) for their valuable contributions to the discussion of this paper.

References

[1] Utracki LA. In: Klempner D, Sperling LH, Utracki LA, editors. Interpenetrating polymer networks. New York: American Chemical Society; 1994. p. 77–123.
[2] Sperling LH, Mishra V. The current status of interpenetrating polymer networks. Polym Adv Technol 1995;7:197–208.
[3] Widmaier JM. Microphase separation during the concurrent formation of two polymer networks. Macro Symp 1995;93:179–86.
[4] Dean K, Cook WD. Azo initiator selection to control the curing order in epoxy/dimethacrylate IPNs. Polym Int 2004;53:1305–13.
[5] Dean K, Cook WD. The effect of curing sequence on the photopolymerization and thermal curing kinetics of dimethacrylate-epoxy interpenetrating polymer networks. Macromolecules 2002;35:7942–54.
[6] Lipatov YS. In: Klempner D, Sperling LH, Utracki LA, editors. Interpenetrating polymer networks. New York: American Chemical Society; 1994. p. 125–39.
[7] Chou YC, Lee LJ. Mechanical properties of polyurethane-unsaturated polyester interpenetrating polymer networks. Polym Eng Sci 1995;35:976–88.
[8] Verchere D, Sautereau H, Pascault JP, Moschiar SM, Riccardi CC, Williams RJJ. In: Keith Riew C, Kinloch AJ, editors. Toughened plastics I science and engineering, vol. 233. Washington DC: American Chemical Society; 1993. p. 336–63.
[9] Suther B, Xiao HX, Klempner D, Frisch KC. In: Kim SC, Sperling LH, editors. IPNs around the world: science and engineering. New York: John Wiley and Sons; 1997. p. 49–73.
[10] Zhou P, Frisch HL, Rogovina L, Makarova L, Zhdanov A, Sergeienko N. Interpenetrating polymer networks of poly-(dimethyl siloxane–urethane) and poly (methyl methacrylate). J Polym Sci A Polym Chem 1993;31:2481–91.
[11] Dubuisson A, Ades D, Fontanille M. Homogeneous epoxy–acrylic interpenetrating polymer networks: preparation and thermal properties. Polym Bull 1980;3:391–8.
[12] Lin MS, Liu CC, Lee CT. Toughened interpenetrating polymer network materials based on unsaturated polyester and epoxy. J Appl Polym Sci 1999;72:585–92.
[13] Frisch HL, Frisch KC, Klempner D. Glass transitions of topologically interpenetrating polymer networks. Polym Eng Sci 1974;14:646–50.
[14] Higgins JS, Benoit HC. Polymers and neutron scattering. In: Lovesey SW, Mitchell EWJ, editors. Oxford series on neutron scattering in condensed matter. New York: Oxford University Press; 1996 [chapter 1].
[15] Bucknall DG, Arrighi V. Neutron scattering of polymer blends. In: Paul DR, Bucknall CB, editors. Polymer blends. New York: Wiley; 2000.
[16] King S. In: Penthrick RA, Dawkins JV, editors. Modern techniques for polymer characterization. New York: John Wiley and Sons; 1999. p. 171–232.
[17] Deybe P, Bueche AM. Scattering by an inhomogeneous solid. J Appl Phys 1949;20:518–26.
[18] Junker M, Alig I, Frisch HL, Fleischer G, Schulz M. Small angle X-ray scattering by simultaneous interpenetrating polymer networks: composition and temperature dependence. Macromolecules 1997;30:2085–91.
[19] Lal J, Widmaier JM, Bastide J, Boue F. Determination of an interpenetrating network structure by small-angle neutron scattering. Macromolecules 1994;27:6443–51.
[20] Higgins JS, Benoit HC. Polymers and neutron scattering. In: Lovesey SW, Mitchell EWJ, editors. Oxford series on neutron scattering in condensed matter. New York: Oxford University Press; 1996. p. 239. and 286.
[21] Cook WD. Fracture and Structure of highly crosslinked polymer composites. J Appl Polym Sci 1991;42:1259–61.
[22] Critchfield FE, Funk GL, Johnson JB. Determination of alpha, beta-unsaturated compounds by reaction with morpholine. Anal Chem 1956;28:76–9.
[23] Dean K, Cook WD, Zipper MD, Burchill P. Curing behaviour of IPNs formed from model VERs and epoxy systems I amine cured epoxy. Polymer 2001;42:1345–59.
[24] Cook WD. Rubber elasticity in relation to polyester networks. Euro Polym J 1977;14:721–7.
[25] Shan L, Robertson CG, Verghese KNE, Burts E, Riffle JS, Ward TC, et al. Influence of vinyl ester/styrene netwrok structure on thermal and mechanical behaviour. J Appl Polym Sci 2001;80:917–27.
[26] Williams JG. Beta relaxation in epoxy resin-based networks. J Appl Polym Sci 1979;23:3433–44.
[27] Ochi M, Okazaki M, Shimbo M. Mechanical relaxation mechanism of epoxide resins cured with alphatic diamines. J Polym Sci Poly Phys Ed 1982;20:689–99.

[28] Ochi M, Iesako H, Shimbo M. Mechanical relaxation mechanism of epoxide resin cured with acid anhydride. II Effect of the chemical structure of the anhydrides on the beta relaxation mechanisms. J Polym Sci B Polym Phys 1986;24: 251–61.

[29] Dean K, Cook WD. The effect of curing sequence on the photopolymerization and thermal curing kinetics of dimethacrylate-epoxy interpenetrating polymer networks. Macromolecules 2002;35:7942–54.